Reducing Cyclic Dispersion in Autoignition Combustion by Controlling Fuel Injection Timing

Erik Hellström, Anna G. Stefanopoulou, and Li Jiang

***Abstract*— Model-based control design for reducing the cyclic variability (CV) in lean autoignition combustion is presented. The design is based on a recently proposed control-oriented model that captures the experimental observations of CV. The model is extended here to include the effect of the fuel injection timing, which is an effective way of influencing the combustion phasing. This model is only stable for certain amounts of residual gas. For high amounts, runaway behavior occurs where the combustion phasing occurs increasingly earlier. For low amounts, a cascade of period-doubling bifurcations occurs leading to chaotic behavior. This complex dynamics is further complicated with significant levels of noise, which creates a challenging control problem. With the aim at controllers feasible for on-board implementation, a proportional controller and a reduced-order state feedback controller are designed, with feedback from the combustion phasing. The controllers are evaluated by simulations and the results show that the CV can be significantly reduced, in an operating point of engine speed and load, for a wide range of residual gas fractions.**

I. Introduction

Cyclic variability (CV) in autoignition combustion, also called homogeneous charge compression ignition (HCCI), is one factor that limits the operating range of such combustion concepts in commercial engines. Recently, a control-oriented model has been developed [1], [2] that captures the experimentally observed evolution of the combustion phasing for high CV when operating HCCI lean (with excess air) with recycling of residual gases through negative valve overlap (nvo). Stability analysis of the model shows that limit cycles and chaotic dynamics appear when reducing the residual gas fraction, and that runaway behavior appear for high amounts of residual gas fraction [2]. Moreover, there are fluctuations in the amount of residuals that appear to be random and that significantly affect the dynamic evolution [2], [3].

The approach here is to control the timing of the fuel injection during the nvo period, using combustion phasing feedback, for reducing the CV. Using injection during nvo for the purpose of control was mentioned [4] and experimentally investigated in [5], [6]. It was used in [7], [8] to extend the low load limit of HCCI. Feedback control for reducing CV was developed in [9] using the injection timing whereas valve timings were modified on a per-cycle basis in [10], [11]. This work is a continuation of [1], [2] and pursues model-based control design for this interesting problem where deterministic instabilities are mixed with stochastic noise. The instabilities appear in the deterministic nonlinear dynamics, governed by the thermal and the chemical coupling between cycles, that are driven by random variations in the residual gas fraction.

E. Hellström and A. G. Stefanopoulou are with the Department of Mechanical Engineering, University of Michigan, Ann Arbor, MI USA (e-mail: {erikhe,annastef}@umich.edu). L. Jiang is with Robert Bosch LLC, Farmington Hills, MI USA (e-mail: li.jiang@us.bosch.com).

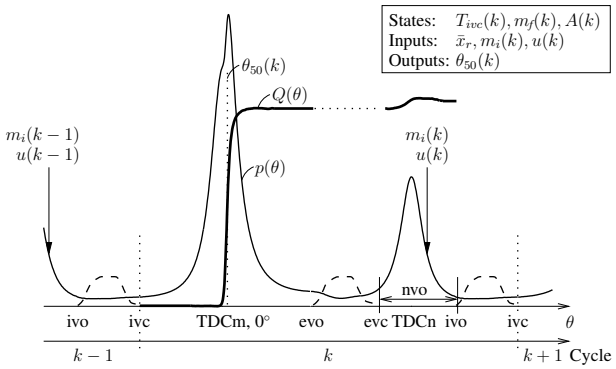

Fig. 1. The engine cycle and key variables for typical cylinder pressure $p(\theta)$, heat release $Q(\theta)$, and valve lift (dashed). The states are the values at ivc for the temperature T_{ivc}, the fuel mass m_f, and the ignition scaling A. The inputs are the mean residual gas fraction $\bar{x}_r$, injection mass m_i, and injection timing u. The problem studied is to control $u(k)$ based on feedback from the combustion phasing $\theta_{50}(k)$ with the goal to reduce CV.

High CV in spark-ignition combustion, which is a related problem although clearly different from CV in HCCI, was reduced in [12] by manipulating the injected fuel mass.

In the next sections, the combustion model from [1], [2] is extended to include the effect of injection timing and the control problem is discussed. After that, the controllers are designed and evaluated by numerical simulation.

II. Combustion model

The model presented in [1], [2] captures the recycling of the thermal and chemical energy in the residual gas and utilizes two states, namely the temperature, $T_{ivc}(k)$, at intake valve closing (ivc) and the fuel amount, $m_f(k)$, in the beginning of cycle k. The model takes into account that combustion efficiency varies with combustion phasing and that heat release can occur during both closed portions of the cycle. The inputs are the mean residual gas fraction, $\bar{x}_r$, and the injected fuel mass, $m_i(k)$. The model is extended here to capture the effect of injection timing. To do this, the crank angle of the injection, denoted by u, is considered as a controlled input and an additional state, denoted by A, is introduced. The definition of the engine cycle and important variables in the model are shown in Fig. 1. In the following, the model from [1], [2] is summarized and the extensions are described.

A. Ignition model

The autoignition process is a complex function of the thermodynamic state and the chemical composition in the cylinder

but, with constant injection timing, the bulk temperature of the cylinder charge has shown to be the dominating effect [13]. The influence on the ignition from fuel injection during nvo is determined by competing thermal and chemical effects [14]. It is assumed here that the conditions are moderately lean so that pyrolysis (breakdown of the fuel molecules) dominates while there is no reforming and subsequent oxidation into final products. Under such conditions, the influence of the injection timing on the combustion phasing of the following combustion was found to be described by an S-shaped curve in the experiments in [15]. This qualitative feature is incorporated in the ignition model from [1], [2].

The crank angle timing of the main combustion, θ_m, is given by an Arrhenius expression whereas the timing for the combustion during re-compression is constant. The ignition delay for the main combustion is given by

$$\tau = A(u)p(\theta)^n \exp\big(B/T(\theta)\big) \tag{1}$$

where $A(u)$ is the state capturing the effect of injection timing, u, and (B,n) are constant tuning parameters. The model (1) is more commonly used without the effect of u with $A(u)$ being a constant [1], [2], [16], [17]. The pressure $p(\theta)$ and temperature $T(\theta)$ are given by polytropic processes,

$$p(\theta) = p_{ivc}\left(\frac{V(\theta_{ivc})}{V(\theta)}\right)^{\gamma} \tag{2a}$$

$$T(\theta) = T_{ivc}\left(\frac{V(\theta_{ivc})}{V(\theta)}\right)^{\gamma-1} \tag{2b}$$

where $V(\theta)$ is the cylinder volume, p_{ivc} is the cylinder pressure at ivc, θ_{ivc} is the crank angle at ivc, and γ is a tuned polytropic exponent. The start of combustion, θ_{soc}, is modeled by the so-called knock-integral approach in [18] and given by $\theta_{soc} = \kappa^{-1}(1)$ where

$$\kappa(\theta_{soc},A) = \int_{\theta_{ivc}}^{\theta_{soc}} \frac{dt}{\tau}, \quad dt = d\theta/\omega \tag{3}$$

and ω is the engine speed. The end of the main combustion, θ_m, is given by

$$\theta_m = \theta_{soc} + \Delta\theta, \quad \Delta\theta = d_1\theta_{soc} + d_0 \tag{4}$$

where $\Delta\theta$ is the burn duration and (d_0,d_1) are tuned parameters. The complete ignition model becomes

$$\theta_m(T_{ivc},A) = \kappa^{-1}(1)\,(1+d_1) + d_0 \tag{5}$$

defined by Eq. (1)–(4).

B. Residual gas fraction

The residual gas fraction x_r is, in practice, mainly regulated by controlling the nvo. Moreover, as shown in [3], the nvo mainly influence the mean value, $\bar{x}_r$, and the variations around the mean can be described by Gaussian white noise,

$$x_r(k) = \bar{x}_r + e(k), \quad e(k) \in N(0,\sigma) \tag{6}$$

where $e(k)$ is normally distributed with zero mean and variance σ^2. One interpretation of Eq. (6) is that it approximates the lumped effect of higher order dynamics, such as turbulent flows, that affects the residual gas fraction in each cycle.

C. Complete model

The structure of the complete model is

$$\begin{cases} T_{ivc}(k+1) = f_1\left(x(k),x_r(k)\right) \\ m_f(k+1) = f_2\left(x(k),x_r(k),m_i(k)\right) \\ A(k+1) = f_3\left(u(k)\right) \end{cases} \tag{7}$$

where $x(k) = \big(T_{ivc}(k),m_f(k),A(k)\big)$ is the state vector and $x_r(k)$ is given by (6). The temperature dynamics f_1, derived in [1], [2], is

$$T_{ivc}(k+1) = (1-x_r(k))T_{im} + x_r(k)T_r(k) \tag{8}$$

where the gas temperature at intake valve opening, $T_r(k)$, is

$$T_r(k) = \Big\{ \alpha\left[1+\beta\,\eta_m(\theta_m)m_f(k)V(\theta_m)^{\gamma-1}\right]^{\frac{1}{\gamma}} + \zeta m_f(k)(1-\eta_m(\theta_m))\Big\}T_{ivc}(k) \tag{9}$$

and (α,β,ζ) are lumped parameters. The combustion efficiency, $\eta_m(\theta_m)$, is modeled by

$$\eta_m(\theta_m) = e_1\left(1+\exp\frac{\theta_m - e_2}{e_3}\right)^{-1}, \tag{10}$$

with the parameters (e_1,e_2,e_3). The end of main combustion $\theta_m = \theta_m(T_{ivc}(k),A(k))$ is defined by (1)–(4). The fuel dynamics f_2 is given by

$$m_f(k+1) = m_i(k) + x_r(k)\,(1-\eta_m(\theta_m))\,(1-\eta_n)\,m_f(k) \tag{11}$$

where η_n is the combustion efficiency during nvo, which is assumed constant. The structure of f_1 and f_2 follows [1], [2] whereas f_3 for the additional state $A(k)$ is introduced for the purpose of modeling the influence of the injection timing $u(k)$ on the ignition in the following cycle. To capture the qualitative characteristics in the experiments in [15], the model is chosen as

$$A(k+1) = s_0 + s_1\left(1+\exp\frac{u(k)}{s_2}\right)^{-1} \tag{12}$$

with the parameters (s_0,s_1,s_2). The injection timing $u(k)$ is given in crank angle degrees, see the illustration in Fig. 2.

The output from the model is the combustion phasing, the 50% burn angle denoted by θ_{50}, and is approximated to occur after half the burn duration. Equation (4) then gives

$$\theta_{50}(k) = \tilde{d}_1\theta_{soc}(T_{ivc}(k),A(k)) + \tilde{d}_0 \tag{13}$$

where $\tilde{d}_0 = d_0/2$ and $\tilde{d}_1 = 1 + d_1/2$.

D. Model parametrization

The model parameters are physically reasonable values taken from the literature. The operating conditions and the geometry, obtained from sensor measurements and engine specifications respectively, are given in Tab. I. With the geometry parameters, the volume V is readily calculated at any crank angle. The parameters specific for the ignition model (1)–(4) are given in Tab. II whereas the parameters for the temperature dynamics f_1 and the fuel dynamics f_2 are

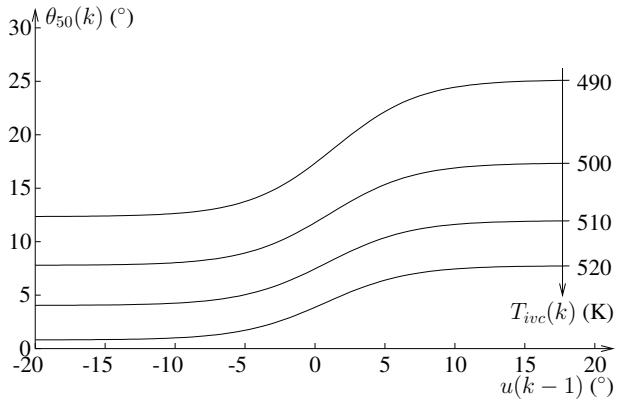

Fig. 2. Ignition model for the effect of injection timing $u(k-1)$ on the combustion phasing $\theta_{50}(k)$ of the following cycle.

given in Tab. III and IV. The parameters for f_3 are given in Tab. V and the model is illustrated in Fig. 2 by computing the output $\theta_{50}(k)$ as a function of $u(k-1)$ for different $T_{ivc}(k)$ using Eq. (12)–(13).

III. Control problem

The inputs to the model in Eq. (7) are $\bar{x}_r$, m_i, and u. The residual gas fraction $\bar{x}_r$ is, as mentioned earlier, regulated by the nvo and, with commercially viable cam phasing mechanisms, this control is on a considerably slower time scale than that of an engine cycle. The injected fuel amount m_i is typically used to track the desired load from the driver. Control of $\bar{x}_r$ and m_i is thus limited by slow actuation and the requirement of tracking the desired load. Therefore, it is here assumed that these are constant and the problem of controlling the injection timing u for reducing the CV is studied. Note, however, that also manipulating m_i on a per-cycle basis should give the same or better performance and may be beneficial if the authority of u is exhausted. In summary, with the additional constant parameters $(\bar{x}_r, m_i)$, the model for the studied control problem is given by Eq. (7) and (6) as

$$\begin{cases} T_{ivc}(k+1) = g_1\left(T_{ivc}(k), m_f(k), A(k), \sigma\right) \\ m_f(k+1) = g_2\left(T_{ivc}(k), m_f(k), A(k), \sigma\right) \\ A(k+1) = g_3\left(u(k)\right) \end{cases} \tag{14}$$

where both the deterministic case ($\sigma = 0$) and the stochastic case ($\sigma > 0$) are studied in the following. The feedback signal is the combustion phasing θ_{50}. This angle, e.g. calculated from in-cylinder pressure sensors, is a suitable signal to use in closed-loop control [19]. Finally, for practical implementation, the controller needs to be simple to make the computation of $u(k)$ based on the calculated $\theta_{50}(k)$, see Fig. 1, feasible in an on-board control unit.

A. Open-loop characteristics

The stability analysis in [2] of the open-loop characteristics, Eq. (14) with $u(k) = 0$ and $\sigma = 0$, shows that the model is only stable for a range of residual gas fractions. This is illustrated in Fig. 3, which show the multipliers (μ_1, μ_2) (the poles corresponding to g_1 and g_2 of the linearized system) for varying $\bar{x}_r$ for a constant load. For high amounts of residuals, runaway behavior occurs where the combustion phasing occurs increasingly earlier. For low amounts, a cascade of period-doubling bifurcations occurs, which eventually leads to seemingly chaotic behavior. These characteristics are shown in the (light gray) orbit diagram in Fig. 4. Also shown are the diagrams for the controllers designed in the next section. Note that the orbit diagram shows the output (13) corresponding to stable fixed points or stable cycles for the model (14) when such exist, which is the case for $\bar{x}_r$ between 42.7% and 54.1%. For $\bar{x}_r$ below 42.7%, there are no stable orbits and 100 iterations of the model are shown.

TABLE I

Quantities known by design or measurements.

Parameter	Symbol	Value
Engine speed	ω	2000 rpm
Intake valve closing	ivc	200 °aTDCn
Pressure at ivc	p_{ivc}	1.08 bar
Intake temperature	T_{im}	300 K
Compression ratio	r_c	12:1
Bore	b	86 mm
Crank radius	a	43 mm
Connecting rod	l	146 mm

TABLE II

Ignition delay and burn duration characteristics.

Parameter	Symbol	Value
Temperature factor	B	$6.3{\cdot}10^3$ K
Pressure exponent	n	-1.4
Burn duration offset	d_0	8 °aTDCm
Burn duration slope	d_1	1.6

TABLE III

Lumped parameters for the temperature dynamics.

Parameter	Symbol	Value
Breathing parameter	α	0.75
Temperature rise factor, main comb.	β	2.0 $^1/_{\text{mg m}^{3(\gamma-1)}}$
Polytropic exponent	γ	1.3
Temperature rise factor, nvo comb.	ζ	0.11 $^1/_{\text{mg}}$

TABLE IV

Efficiency parameters.

Parameter	Symbol	Value
Scaling, main comb. efficiency	e_1	0.99
Shift, main comb. efficiency	e_2	30 °aTDCm
Slope, main comb. efficiency	e_3	6.5 °
Efficiency for nvo comb.	η_n	80 %

TABLE V

Injection timing parameters.

Parameter	Symbol	Value
Offset parameter	s_0	2200 $^{\text{mg}}/_{\text{bar}^n}$
Scaling parameter	s_1	600 $^{\text{mg}}/_{\text{bar}^n}$
Slope parameter	s_2	3 °

IV. Controller design

Controller design based on the model in Eq. (14) is carried out for one operating point corresponding to an engine speed of 2000 rpm and a load given by m_i of 12 $^{\text{mg}}/_{\text{cycle}}$. The design is done in a deterministic setting, $\sigma = 0$, whereas noise is

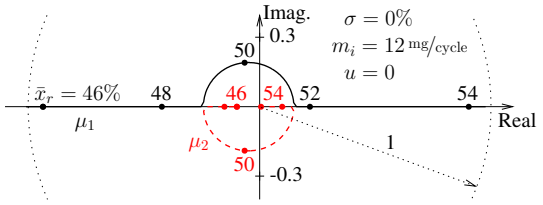

Fig. 3. Locus of the open-loop multipliers (μ_1, μ_2) for varying $\bar{x}_r$ between 45.7% (first period-doubling occurs) and 54.1% (runaway occurs).

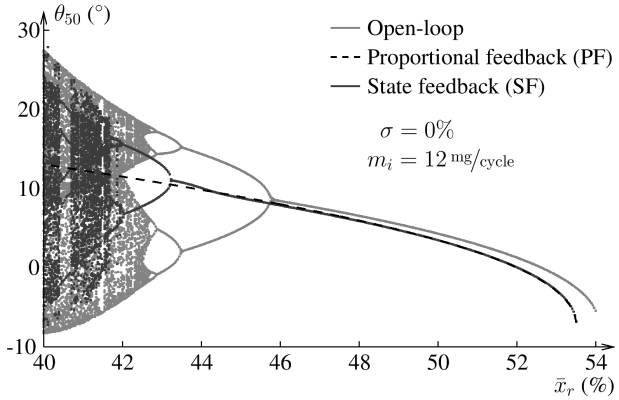

Fig. 4. Orbit diagrams for the combustion phasing θ_{50} for the system in open-loop and in closed-loop with the controllers designed in Sec. IV.

considered in the evaluation of the controller performance.

A. Proportional control

Proportional feedback control was proposed in the first seminal papers on control of chaotic dynamics [20]–[22]. The controller design methods in these papers do not rely on an explicit model of the system, instead experimental observations are used to estimate a number of key features that determine the gain. Here, the model is utilized to select the gain. A proportional controller, denoted by PF, with feedback from the combustion phasing θ_{50} is

$$u(k) = K(\theta_{50}(k) - \theta^*_{50}) \qquad \text{(PF)}$$

where K is the gain and θ^*_{50} is the desired reference point. To select the gain, the multipliers for the model (14) with $\bar{x}_r = 42\%$ and the control (PF) are computed. The locus of the multipliers are shown in Fig. 5. The two multipliers (μ_1, μ_2)

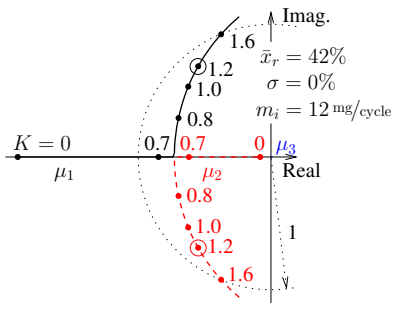

Fig. 5. Locus of the closed-loop multipliers (μ_1, μ_2, μ_3) for varying feedback gain K with proportional control. The choice of $K = 1.2$ encircled.

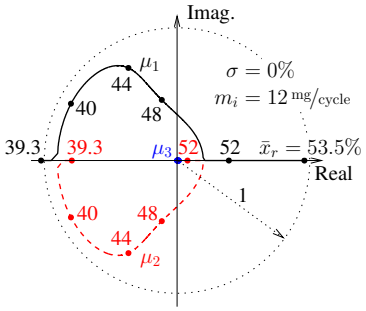

Fig. 6. Locus of the closed-loop multipliers (μ_1, μ_2, μ_3) varying residual gas fraction $\bar{x}_r$ with the proportional gain $K = 1.2$.

move from their open-loop locations as K increases and indicate a stable system for K between 0.7 and 1.6. The third multiplier μ_3 has a small non-negative real value for all K. A value of $K = 1.2$ is selected as a trade off between oscillation amplitude and settling time in the transient response.

Now, the closed-loop system with $K = 1.2$ and varying residual gas fraction is analyzed. The multipliers, shown in Fig. 6, show that the control successfully stabilizes the system for $\bar{x}_r$ between 39.3% and 53.5%. The steady-state behavior is shown in Fig. 4. The limit cycles and the chaotic dynamics are stabilized and reduced to a stable fixed point for $\bar{x}_r$ larger than 39.3% whereas the point of runaway is moved to a slightly lower $\bar{x}_r$, from $\bar{x}_r$ 54.1% to 53.5%.

B. State feedback control

With state feedback control, there are more parameters to tune and, naturally, more flexibility in the design of the closed-loop dynamics. Here, the well known linear techniques with a Kalman filter and a linear-quadratic regulator are used as tools for determining the controller parameters in a systematic way. Thus, Eq. (14) is first linearized and the states are normalized to obtain a linear model,

$$\begin{aligned} \tilde{x}(k+1) &= A\tilde{x}(k) + B\delta u(k) \\ \delta\theta_{50}(k) &= C\tilde{x}(k) \end{aligned} \qquad (15)$$

where $\tilde{x}$ is the normalized state vector and $(\delta u, \delta\theta_{50})$ are the control and output deviations, respectively, from the nominal point. The point of linearization is the unstable fixed point with input $\bar{x}_r = 44\%, m_i = 12\,\mathrm{mg/cycle}, u = 0°$ corresponding to the state $x = (503.7\,\mathrm{K}, 12.1\,\mathrm{mg}, 2500\,\mathrm{s}\cdot\mathrm{bar}^{1.4})$.

For the observer, the variance for the measurement noise is set to 1 and the covariance matrix for the states is chosen diagonal with the elements (100,1,10). The regulator is designed by minimizing $\sum_{k=1}^{\infty}\left(100\delta\theta_{50}(k)^2 + \delta u(k)^2\right)$. To simplify the controller as much as possible, controller order reduction was performed by computing a balanced realization and removing states with small Hankel singular values. The final controller has one state, is given by

$$\begin{aligned} \xi(k+1) &= \quad 0.6307\,\xi(k) - 1.204\,\delta\theta_{50}(k) \\ \delta u(k) &= -1.204\;\; \xi(k) + 2.002\,\delta\theta_{50}(k) \end{aligned} \qquad \text{(SF)}$$

and is denoted by SF in the following.

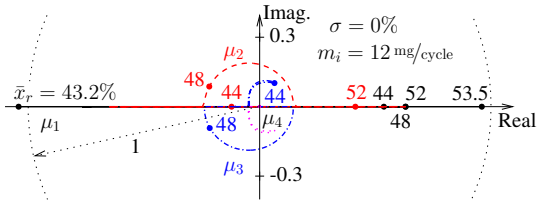

Fig. 7. Locus of the closed-loop multipliers $(\mu_1, \mu_2, \mu_3, \mu_4)$ for varying residual gas fraction x_r with state feedback control. The multipliers (μ_1, μ_2) first move back and forth on the real axis between ± 0.5, for $\bar{x}_r$ between 43.2% and 46.4%, and then moves right towards 1 for higher $\bar{x}_r$ while (μ_3, μ_4) moves around close to the origin.

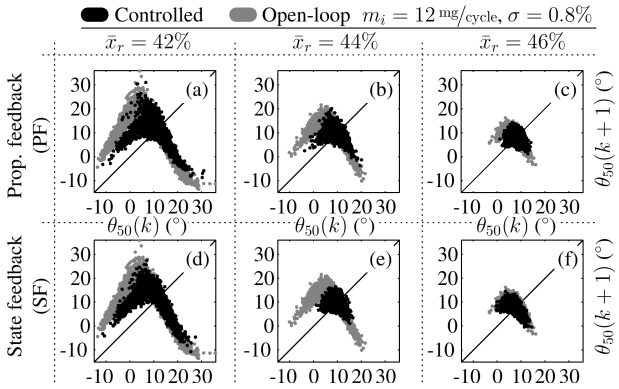

Fig. 8. Return maps for 3000 cycles. The PF shows fairly good performance in (b)–(c) whereas the performance with the SF deteriorates away from the nominal point. The case in (a) and (d) is challenging for both controllers due to the very low residual gas fraction.

Figure 7 shows the closed-loop multipliers for varying $\bar{x}_r$ using the controller (SF), and Fig. 4 shows the steady state behavior. The control successfully stabilizes the system between 43.2% and 53.5%. The stable period-4 and period-2 cycles for $\bar{x}_r$ between 43.2% and 45.7%, see Fig. 4, are reduced to a stable fixed point. The closed-loop is not stable below $\bar{x}_r$ of 43.2% and the behavior when reducing $\bar{x}_r$ is similar to the open-loop although the amplitudes of the first stable limit cycles are reduced. Compared to the proportional control, the stability region for the state feedback is narrower in $\bar{x}_r$ but the locations of the multipliers, e.g., indicate a more damped transient response in the nominal point of $\bar{x}_r = 44\%$.

V. Controller Evaluation

To evaluate the controllers in a realistic setting, noise is introduced. As shown in [1]–[3], the model (14) is representative of the open-loop behavior observed in experiments and the level of noise is approximately $\sigma = 0.8\%$. The PF and

TABLE VI

Mean and standard deviation of the combustion phasing $(\bar{\theta}_{50}, \sigma_{50})$ in open loop and with feedback control.

	$\bar{x}_r = 42\%$		$\bar{x}_r = 44\%$		$\bar{x}_r = 46\%$	
	$\bar{\theta}_{50}$	σ_{50}	$\bar{\theta}_{50}$	σ_{50}	$\bar{\theta}_{50}$	σ_{50}
Open loop	8.8	9.5	8.9	5.4	8.1	2.7
Prop. feedback	10.8	4.9	9.6	2.6	7.9	1.8
State feedback	10.7	5.5	9.8	2.0	7.7	2.1

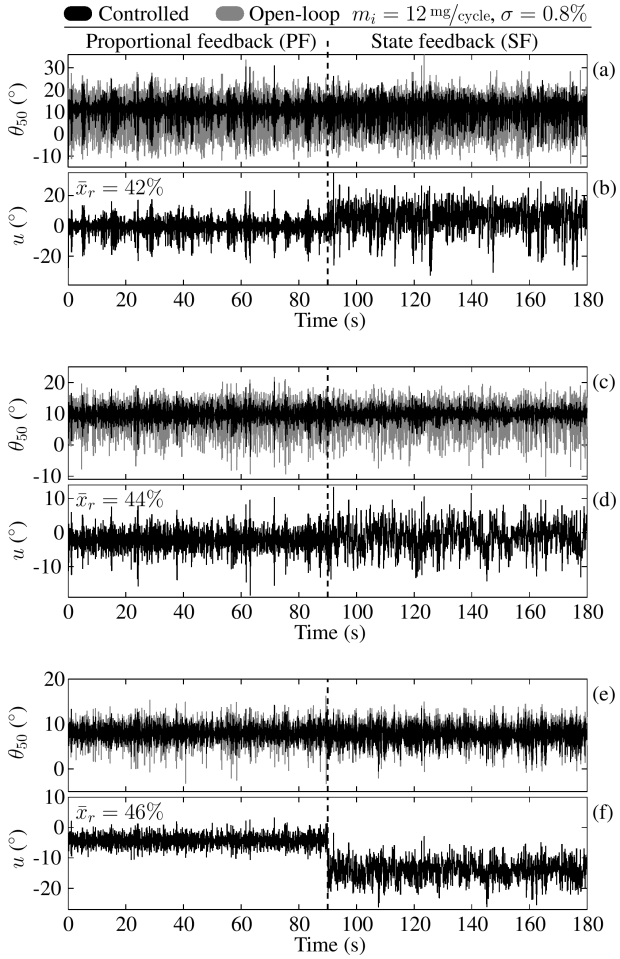

Fig. 9. The time evolution of the output, θ_{50}, and the control, u, for 180 s, where the controller is switched at 90 s. The performance is overall better with the PF than with the SF.

SF controllers are compared in Fig. 8 with the open-loop behavior using the simulated return maps for 3000 cycles for varying $\bar{x}_r$. Table VI shows a comparison in terms of mean and standard deviation of the combustion phasing $(\bar{\theta}_{50}, \sigma_{50})$. The time evolution is shown in Fig. 9 for 3 min, equal to 3000 cycles at 2000 rpm, where the control is switched between the two controllers after half the time.

The characteristic shapes in the return maps for the open-loop cases in Fig. 8 indicate that there are low-order nonlinear deterministic couplings between subsequent cycles [2]. A controller should, ideally, make the variability between cycles purely random, which would manifest itself as featureless clouds in the return maps. Both controllers do contract the pattern in all cases. Table VI shows that the standard deviation of the combustion phasing, σ_{50}, is reduced by between one fourth and one half of the open loop case while the average values are close to the open-loop case or later. The SF has the best performance for $\bar{x}_r$ of 44%, which is the closest point to the nominal point for the design of the controller. However, when $\bar{x}_r$ is decreased or increased from this point, the performance deteriorates and the PF is better. For the case with the $\bar{x}_r = 42\%$ in Fig. 8(a) and 8(d), both

controllers contract the pattern slightly but there are still clear deterministic couplings between cycles. This case is expected to be the most challenging due to the underlying chaotic dynamics in the model that is mixed with stochastic noise. Figures 9(a)–(b) show that with PF, unlike with SF, the CV is reduced during periods of time but there are spurious burst with higher CV. The PF stabilizes the chaos at $\bar{x}_r = 42\%$ in the absence of noise, as shown in Fig. 4, but a realistic noise level leads to such bursts. With SF, the closed-loop is not stable at this $\bar{x}_r$ and the performance is poor despite reduced noise. With PF, u is mostly in between $\pm 10^\circ$, see Fig. 9, where there is still control authority left, see Fig. 2, although there are a few spikes towards $\pm 20^\circ$. The SF also utilizes a reasonable range of the actuator except for the case with $\bar{x}_r$ of 46% as shown in Fig. 9(e)–(f).

VI. Conclusions

Feedback controllers for reducing CV in autoignition combustion are designed and evaluated by numerical simulation. A proportional control of the injection timing with feedback from the combustion phasing is shown to perform well for an operating point (engine speed and load) with a wide range of residual gas fractions. Without noise, this controller increases the stable range of the combustion by stabilizing the limit cycles and the chaotic dynamics associated with low amounts of residual gas fraction. The CV is still reduced when adding noise with magnitude observed in experiments. The performance deteriorates, however, for values of the residual gas fraction in the chaotic region. A state feedback controller is designed using linear techniques, which improves upon the proportional feedback close to the nominal conditions but worsens the performance for other conditions. Future work pertains to experimental evaluation of the controllers.

Acknowledgments

This material is based upon work supported by the Department of Energy (National Energy Technology Laboratory) under award number DE-EE0003533 and performed as a part of the ACCESS project consortium (Robert Bosch LLC, AVL Inc., Emitec Inc.) under the direction of PI Hakan Yilmaz, Robert Bosch, LLC.[1] E. Hellström also gratefully acknowledges the award from Bernt Järmark's Foundation for Scientific Research.

References

[1] E. Hellström and A. G. Stefanopoulou. Modeling cyclic dispersion in autoignition combustion. In *Proc. 50th IEEE Conference on Decision and Control*, pages 6834–6839, 2011.

[1] Disclaimer: This report was prepared as an account of work sponsored by an agency of the United States Government. Neither the United States Government nor any agency thereof, nor any of their employees, makes any warranty, express or implied, or assumes any legal liability or responsibility for the accuracy, completeness, or usefulness of any information, apparatus, product, or process disclosed, or represents that its use would not infringe privately owned rights. Reference herein to any specific commercial product, process, or service by trade name, trademark, manufacturer, or otherwise does not necessarily constitute or imply its endorsement, recommendation, or favoring by the United States Government or any agency thereof. The views and opinions of authors expressed herein do not necessarily state or reflect those of the United States Government or any agency thereof.

[2] E. Hellström, A. G. Stefanopoulou, and L. Jiang. Cyclic variability and dynamical instabilities in autoignition engines with high residuals. 2012. Submitted to the IEEE Trans. Control Syst. Technol.

[3] E. Hellström, A. G. Stefanopoulou, J. Vávra, A. Babajimopoulos, D. Assanis, L. Jiang, and H. Yilmaz. Understanding the dynamic evolution of cyclic variability at the operating limits of HCCI engines with negative valve overlap. In *SAE World Congr.*, 2012. SAE 2012-01-1106.

[4] J. Willand, R-G. Nieberding, G. Vent, and C. Enderle. The knocking syndrome–its cure and its potential. In *SAE Int. Fall Fuels and Lubricants Meeting and Exhibition*, 1998. SAE 982483.

[5] L. Koopmans, H. Ström, S. Lundgren, O. Backlund, and I. Denbratt. Demonstrating a SI-HCCI-SI mode change on a Volvo 5-cylinder electronic valve control engine. In *SAE World Congr.*, 2003. SAE 2003-01-0753.

[6] T. Urushihara, K. Hiraya, A. Kakuhou, and T. Itoh. Expansion of HCCI operating region by the combination of direct fuel injection, negative valve overlap and internal fuel reformation. In *SAE World Congr.*, 2003. SAE 2003-01-0749.

[7] H. H. Song, A. Padmanabhan, N. B. Kaahaaina, and C. F. Edwards. Experimental study of recompression reaction for low-load operation in direct-injection homogeneous charge compression ignition engines with n-heptane and i-octane fuels. *Int. J. Engine Res.*, 10(4):215–229, 2009.

[8] N. Wermuth, H. Yun, and P. Najt. Enhancing light load HCCI combustion in a direct injection gasoline engine by fuel reforming during recompression. *SAE Int. J. Engines*, 2(1):823–836, 2009.

[9] A. F. Jungkunz, H.-H. Liao, N. Ravi, and J. C. Gerdes. Combustion phasing variation reduction for late-phasing HCCI through cycle-to-cycle pilot injection timing control. In *Proc. ASME Dynamic Systems and Control Conference*, 2011. DSCC2011-6091.

[10] N. Ravi, M. J. Roelle, H.-H. Liao, A. F. Jungkunz, C.-F. Chang, S. Park, and J. C. Gerdes. Model-based control of HCCI engines using exhaust recompression. *IEEE Trans. Control Syst. Technol.*, 18(6):1289 –1302, 2010.

[11] A. F. Jungkunz, H.-H. Liao, N. Ravi, and J. C. Gerdes. Reducing combustion variation of late-phasing HCCI with cycle-to-cycle exhaust valve timing control. In *IFAC Symp. on Advances in Automotive Control*, 2010.

[12] L. I. Davis, Jr., L. A. Feldkamp, J. W. Hoard, F. Yuan, F. T Connolly, C. S. Daw, and J. B. Green, Jr. Controlling cyclic combustion variations in lean-fueled spark-ignition engines. In *SAE World Congr.*, 2001. SAE 2001-01-0257.

[13] C. J. Chiang and A. G. Stefanopoulou. Sensitivity analysis of combustion timing of homogeneous charge compression ignition gasoline engines. *J. Dyn. Syst. Meas. Contr.*, 131(1):014506, 2009.

[14] H. H. Song and C. F. Edwards. Understanding chemical effects in low-load-limit extension of homogeneous charge compression ignition engines via recompression reaction. *Int. J. Engine Res.*, 10(4):231–250, 2009.

[15] N. Ravi, H.-H. Liao, A. F. Jungkunz, and J. C. Gerdes. Modeling and control of exhaust recompression HCCI using split injection. In *Proc. American Control Conference*, pages 3797–3802, 2010.

[16] F. Agrell, H.-E. Ångström, B. Eriksson, J. Wikander, and J. Linderyd. Integrated simulation and engine test of closed loop HCCI control by aid of variable valve timings. In *SAE World Congr.*, 2003. SAE 2003-01-0748.

[17] D. J. Rausen, A. G. Stefanopoulou, J.-M. Kang, Eng J. A., and T.-W. Kuo. A mean-value model for control of homogeneous charge compression ignition (HCCI) engines. *J. Dyn. Syst. Meas. Contr.*, 3(3):355–362, 2005.

[18] J. C. Livengood and P. C. Wu. Correlation of autoignition phenomena in internal combustion engines and rapid compression machines. In *5th Int. Symp. on Combustion*, pages 347–356, 1955.

[19] J. Bengtsson, P. Strandh, R. Johansson, P. Tunestål, and B. Johansson. Closed-loop combustion control of homogeneous charge compression ignition (HCCI) engine dynamics. *Int. J. Adapt. Control Signal Process.*, 18(2):167–179, 2004.

[20] E. Ott, C. Grebogi, and J. A. Yorke. Controlling chaos. *Phys. Rev. Lett.*, 64(11):1196–1200, 1990.

[21] B. Peng, V. Petrov, and K. Showalter. Controlling chemical chaos. *J. Phys. Chem.*, 95(13):4957–4959, 1991.

[22] V. Petrov, V. Gaspar, and J. Masere. Controlling chaos in the Belousov-Zhabotinsky reaction. *Nature*, 1993.